

Semiclassical and quantum shell-structure calculations of the moment of inertia

D.V. Gorpchenko,¹ A.G. Magner,^{1,*} and J. Bartel²

¹*Institute for Nuclear Research, 03680 Kyiv, Ukraine*

²*Institut Pluridisciplinaire Hubert Curien, CNRS/IN2P3,*

Université de Strasbourg, F-67000 Strasbourg, France

(Dated: March 11, 2020)

Shell corrections to the moment of inertia (MI) are calculated for a Woods-Saxon potential of spheroidal shape. For the statistical equilibrium collective rotations under consideration, the MI is obtained within the cranking model in an approach which goes beyond the quantum perturbation approximation based on the non perturbative energy spectrum. For the calculation of the MI shell corrections $\delta\Theta$, the Strutinsky smoothing procedure is used to obtain the average occupation numbers of the particle density using the solutions of the Woods-Saxon eigenvalue problem. We find that the major-shell structure of $\delta\Theta$ is generated by the same inhomogeneity of the distribution of single-particle states near the Fermi surface as the energy shell corrections δE . This fundamental property is in agreement with the semiclassical results $\delta\Theta \propto \delta E$ obtained analytically within the periodic orbit theory for any potential well, in particular for the spheroidal cavity.

PACS numbers: 21.10. Ev, 21.60. Cs, 24.10 Pa

I. INTRODUCTION

Many significant phenomena in nuclear rotations can be explained within the theoretical approaches based on the cranking model [1–5], and the Strutinsky shell-correction method (SCM) [6, 7]. This approach was extended by Pashkevich and Frauendorf [8, 9] to the description of collective rotational bands. For a deeper understanding of the correspondence between the classical and the quantum approach and their applications to high-spin physics, it is worthwhile to analyze the shell components of the moment of inertia (MI) within the semiclassical periodic-orbit theory (POT) [10–20]. The cranking model is, to some extent, of semiclassical nature because the collective rotation of the nuclear many-body systems is described as a classical transformation from the laboratory to the body-fixed coordinate system, rotating around the former with fixed angular velocity [4, 5]. Using this semiclassical picture, one can reduce the complex problem of the rotation of a many-body system to a much simpler diagonalization of an effective mean-field (one-body) Hamiltonian in the rotating frame. In the semiclassical limit of large particle numbers ($\hbar/S \sim N^{-1/3} \rightarrow 0$, where S is the action integral that includes all POs that give any significant contribution) one can neglect the energy distances between nearest-neighbor quantum states. In this limit the energy spectrum of the unperturbed Hamiltonian (without rotation) can be considered as quasi-continuous, and, therefore, any finite rotational excitations could never be considered as small as compared with the distances between non perturbative neighboring levels, thus violating the condition of applicability of the quantum perturbation expansion. One could, however, consider another

perturbation approach based on the concept of a statistical equilibrium rotation with a generalized rigid-body (GRB) moment of inertia Θ_{GRB} [21] (see Refs. [19, 22–26]),

$$\Theta \approx \Theta_{\text{GRB}} = m \int d\mathbf{r} r_{\perp}^2 \rho(\mathbf{r}), \quad (1)$$

where m is the nucleon mass, r_{\perp} the distance between a given point \mathbf{r} of the nucleus and the rotation axis, and $\rho(\mathbf{r}) = \tilde{\rho} + \delta\rho(\mathbf{r})$ the one-body quantum particle-number density. According to the SCM [6, 7], $\tilde{\rho}$ is a smooth density and $\delta\rho(\mathbf{r})$ its shell correction. It is obviously this shell component $\delta\rho(\mathbf{r})$ which determines the MI shell correction $\delta\Theta \approx \delta\Theta_{\text{GRB}}$.

The semiclassical perturbation expansion [16, 27] by Greagh has been used in the POT calculations of the MI shell corrections for a spheroidal cavity mean field [28]. The non perturbative Gutzwiller POT, extended to the bifurcation phenomena at large deformations [20, 29–31], on the other hand, was applied [25] within the cranking model and a harmonic-oscillator mean field to describe collective rotations (around an axis perpendicular to the symmetry axis). For adiabatic collective rotations (rotations at statistical equilibrium) the MI is then described as the sum of a smooth Extended Thomas-Fermi (ETF) MI Θ_{ETF} [22, 32] and shell corrections $\delta\Theta$ [19, 22–24]. In a more realistic description of the MI for collective rotations, the ETF approach has already been successful, as in the case of the nuclear energy [33], by including self-consistency and spin effects into the calculations [22, 32].

As shown in Refs. [19, 22–24], one can obtain, through a semiclassical phase-space trace formula, with a good approximation, analytical expressions for MI shell components $\delta\Theta$ in terms of the energy shell corrections δE , for an arbitrary potential well,

$$\delta\Theta \propto \delta E, \quad (2)$$

a relation which has been worked out for integrable Hamiltonians, such as for a harmonic oscillator [22, 25]

* Email: magner@kinr.kiev.ua

or a spheroidal-cavity [19, 23, 24] mean field. Corrections accounting for a finite surface diffuseness and finite temperature effects of the nuclear system can also been taken into account as demonstrated in Refs. [24] and [19], respectively. The exponential decrease of the MI shell corrections $\delta\Theta$ with increasing temperature and the possibility to express $\delta\Theta$ through the free-energy shell corrections δF have in particular been discussed in Ref. [19]. For the deformed Woods-Saxon (WS) potential well (of spheroidal type) with large depth and small surface diffuseness, as already considered in Refs. [14, 31], we are going, in the present study, to compare the quantum MI shell corrections $\delta\Theta$ with the energy shell corrections calculated both by the SCM, which will allow us to assess the validity of the semiclassical POT relationship (2) [19, 22, 24, 25].

II. MI SHELL CORRECTIONS

A. The cranking model

Collective rotations of a Fermi system associated with a many-body Hamiltonian can be described in the mean-field approximation by the cranking model. The complex problem of a rotating many-body Fermi system can then be reduced, in the restricted subspace of Slater determinants, to a much simpler eigenvalue problem of a single-particle (s.p.) Hamiltonian

$$\hat{\mathcal{H}}^\omega = \hat{\mathcal{H}} - \boldsymbol{\omega} \cdot \hat{\boldsymbol{\ell}} = \hat{\mathcal{H}} - \omega \cdot \hat{\ell}_x, \quad (3)$$

where $\hat{\boldsymbol{\ell}}$ is the s.p. angular-momentum operator with component $\hat{\ell}_x$, having defined $0x$ as rotation axis perpendicular to the symmetry $0z$ axis. The Hamiltonian (3) is usually referred to as the *Routhian*. For simplicity, we shall discard the spin and isospin degrees of freedom, in particular the spin-orbit and asymmetry interactions. The rotation frequency ω of the body-fixed coordinate system with respect to the laboratory frame is the Lagrange multiplier of our problem, associated with the constraint on the nuclear angular momentum I_x . The angular velocity ω needs to be adjusted in such a way that the quantum average $\langle \hat{\ell}_x \rangle^\omega$ of the s.p. orbital angular-momentum operator $\hat{\ell}_x$ yields the required angular momentum I_x . This quantum average is obtained in a similar way as the expectation value of the many-body Routhian (3) in the subspace of Slater determinants,

$$\langle \hat{\ell}_x \rangle^\omega \equiv d_s \sum_i n_i^\omega \int d\mathbf{r} \psi_i^\omega(\mathbf{r}) \hat{\ell}_x \bar{\psi}_i^\omega(\mathbf{r}) = I_x, \quad (4)$$

where d_s is the spin (spin-isospin) degeneracy of the s.p. states, n_i^ω their occupation numbers, with corresponding eigenvalues ε_i^ω and eigenfunctions $\psi_i^\omega(\mathbf{r})$ of \hat{H}^ω , Eq. (3), and $\bar{\psi}_i^\omega(\mathbf{r})$ their complex conjugate. For relatively small angular velocities ω (neglecting terms non-linear in

ω) and at zero nuclear temperature, the chemical potential λ^ω is, to a good approximation, equal to the Fermi energy: $\lambda^\omega \approx \varepsilon_F = \hbar^2 k_F^2 / 2m$, where $\hbar k_F$ is the Fermi momentum. Within the same approach, one approximately has for the particle number

$$N = d_s \sum_i n_i^\omega \int d\mathbf{r} \psi_i^\omega(\mathbf{r}) \bar{\psi}_i^\omega(\mathbf{r}) \approx d_s \int_0^\infty d\varepsilon n^\omega(\varepsilon), \quad (5)$$

where the occupation numbers $n^\omega(\varepsilon)$ depend on the chemical potential λ^ω which has to be adjusted to obtain the desired particle number N .

B. MI as a collective response

Since the continuous parameter ω is introduced and the uncertainty relation between the angular momentum and the rotation angles of the body-fixed coordinate system is neglected, the cranking model is semiclassical in nature [5, 19, 23, 24]. One may thus consider the collective MI Θ_x , for a rotation around the x axis, as the response of the quantum average $\delta\langle\hat{\ell}_x\rangle^\omega$ to the external cranking field $-\omega\hat{\ell}_x$ in Eq. (3) [18, 19, 22–25, 34–36],

$$\delta\langle\hat{\ell}_x\rangle^\omega = \Theta_x \delta\omega, \quad (6)$$

where

$$\Theta_x = \frac{\partial\langle\hat{\ell}_x\rangle^\omega}{\partial\omega} = \frac{\partial^2 E(\omega)}{\partial\omega^2}, \quad (7)$$

with

$$E(\omega) = \langle \hat{\mathcal{H}}^\omega \rangle \approx E(0) + \frac{I_x^2}{2\Theta_x}. \quad (8)$$

For a nuclear rotation around the x axis, one can treat, as shown in Refs. [1, 3, 4, 8, 9], the term $-\omega\hat{\ell}_x$ as a small perturbation. With the constraint (4) and the MI, Eq. (7), if treated in second-order quantum perturbation theory, one obtains the well-known Inglis cranking formula [1, 4, 5].

For the derivation of the MI shell corrections within the SCM [6, 8, 9], beyond the quantum perturbation approach, it turns out to be helpful to use the coordinate space representation of the MI through the one of the s.p. Green's functions $G(\mathbf{r}_1, \mathbf{r}_2; \varepsilon)$ as this was done for the other transport coefficients in Refs. [19, 25, 34, 36]. Taking advantage of the analogy of our problem of a rotating many-body system with magnetism, where the magnetization \mathbf{M} is proportional to the field strength \mathbf{B} with the magnetic susceptibility χ as the proportionality constant, the MI Θ_x , Eq. (7), can be expressed in a coordinate representation, as a kind of susceptibility, or as the response function for collective vibrations [19], in terms of the Green's function G (see also Refs. [22–24, 34]). For adiabatic rotations, one then has

$$\Theta_x = \frac{2d_s}{\pi} \int_0^\infty d\varepsilon n(\varepsilon) \int d\mathbf{r}_1 \int d\mathbf{r}_2 \ell_x(\mathbf{r}_1) \ell_x(\mathbf{r}_2) \times \text{Re}[G(\mathbf{r}_1, \mathbf{r}_2; \varepsilon)] \text{Im}[G(\mathbf{r}_1, \mathbf{r}_2; \varepsilon)], \quad (9)$$

where $\ell = [\mathbf{r} \times \mathbf{p}]$ is the particle angular momentum. Formally, with the help of the spectral representation of the Green's function $G(\mathbf{r}_1, \mathbf{r}_2; \varepsilon)$, one can also obtain from Eq. (9) the famous Inglis formula for the MI [4, 5].

Within the semiclassical POT, the coordinate representation (9) is extremely useful, since it allows to weaken the applicability criterion of the quantum perturbation approximation, because the leading terms of the POT in expansion over small parameter \hbar/S (S is the action integral for main POs) is related to the statistically averaging over many quantum states. Therefore, the maximal rotational excitation energy $\hbar\omega$ for which the approximation is valid becomes now significantly larger than the nearest-neighbor s.p. level spacing around the Fermi surface ε_F . At the same time, $\hbar\omega$ still remains somewhat smaller than the energy distance between major shells $\hbar\Omega$ ($\hbar\Omega \approx \varepsilon_F/N^{1/3}$) as shown by Migdal [37]. These two conditions are in contrast to the energy spectrum representation of the quantum perturbation approach where, in the derivation of the standard Inglis cranking formula the excitation energies are required to be small with respect to the s.p. level spacing. This more severe restriction is obviously avoided by using the coordinate-space representation of the Green's function G in Eq. (9).

C. Statistically equilibrium rotation

For a semiclassical statistical-equilibrium rotation with constant frequency ω , one approximately obtains [19, 22, 25] Eq. (1) for the MI Θ_x in terms of the GRB MI (to simplify the notation, the sub-script x will be omitted in what follows),

$$\Theta \approx m \int d\mathbf{r} r_{\perp}^2 \rho(\mathbf{r}) = \tilde{\Theta} + \delta\Theta, \quad (10)$$

with $r_{\perp}^2 = y^2 + z^2$ and the smooth part $\tilde{\Theta} = m \int d\mathbf{r} r_{\perp}^2 \tilde{\rho}(\mathbf{r})$ of the MI [19, 22, 23, 25, 32], while the shell correction is given by [19, 22, 23, 25],

$$\delta\Theta = m \int d\mathbf{r} r_{\perp}^2 \delta\rho(\mathbf{r}). \quad (11)$$

Eq. (10) is a local approximation (valid for the statistically averaged rotation [21, 22, 25]) to the general equation (9).

The separation in Eq. (10) of the MI into a smooth (average) part and a shell correction has, of course, its origin in the corresponding subdivision of the spatial particle density

$$\rho(\mathbf{r}) = -\frac{1}{\pi} \text{Im} \int d\varepsilon n(\varepsilon) [G(\mathbf{r}_1, \mathbf{r}_2; \varepsilon)]_{\mathbf{r}_1=\mathbf{r}_2=\mathbf{r}} = \tilde{\rho} + \delta\rho \quad (12)$$

into a smooth part $\tilde{\rho}$ and a shell correction given by

$$\delta\rho(\mathbf{r}) = -\frac{1}{\pi} \text{Im} \int d\varepsilon \delta n(\varepsilon) [G(\mathbf{r}_1, \mathbf{r}_2; \varepsilon)]_{\mathbf{r}_1=\mathbf{r}_2=\mathbf{r}}.$$

Eq. (12) is stemming originally from the standard decomposition of the occupation numbers into smooth and fluctuating (shell) parts as usual in the SCM [7]

$$n = \tilde{n} + \delta n. \quad (13)$$

III. QUANTUM CALCULATIONS

In this section, we will describe a system of independent fermions (nucleons) moving in a deformed mean field of the form of a Woods-Saxon (WS) potential of spheroidal shape with Oz as symmetry axis. One then has to solve the Schrödinger equation with a potential

$$V(r, \theta) = \frac{V_0}{1 + \exp \{[r - R(\theta)]/\alpha\}}, \quad (14)$$

where $R(\theta)$ denotes the radius of the spheroidal surface [19, 38, 39] in spherical coordinates $\{r, \theta, \varphi\}$ and α the surface diffuseness. Introducing semiaxes a and b through the equation

$$(x^2 + y^2)/a^2 + z^2/b^2 = 1, \quad (15)$$

where, because of volume conservation, one must require that $a^2b = R_0^3$, with R_0 the radius of the corresponding spherical shape, one can define through

$$\eta = \frac{b}{a} \quad (16)$$

a deformation parameter that will be larger one for prolate ($b > a$) and smaller one for oblate ($a > b$) shapes.

To solve the Schrödinger (eigenvalue) equation with the potential (14) one can conveniently use the expansion of the WS eigenfunctions in terms of the well-known deformed axially-symmetric harmonic-oscillator (HO) basis [40], as explained in the appendix. The particle number density $\rho(\varrho, z)$ can then be written in cylindrical coordinates $\{\varrho, z, \varphi\}$, where $\varrho = \sqrt{x^2 + y^2}$, in the standard form:

$$\rho(\varrho, z) = \sum_i n_i |\psi_i(\varrho, z, \varphi)|^2, \quad (17)$$

where the WS eigenfunctions $\psi_i(\varrho, z, \varphi)$ are given in terms of the HO eigenfunctions Φ_i (as explained in the appendix, Eq. (A.2)). For the MI of statistical equilibrium rotation one has $\Theta \approx \Theta_{\text{GRB}}$, where

$$\Theta_{\text{GRB}} = m \int d\mathbf{r} r_{\perp}^2 \rho(\varrho, z) = \sum_i n_i \Theta_i \quad (18)$$

with

$$\Theta_i = m \sum_{j,k} A_{ij} A_{ik} \left(J_{jk}^{(y)} + J_{jk}^{(z)} \right). \quad (19)$$

Here $A_{\mu\nu}$ are the expansion coefficients of the WS eigenfunctions (A.1) in the HO basis (see Appendix). In Eq. (19) we also introduced

$$J_{jk}^{(y)} = \int d\mathbf{r} y^2 \Phi_j^*(\mathbf{r}) \Phi_k(\mathbf{r}) = \frac{\hbar}{2m\omega_{\perp}} \delta_{n_z, n'_z} \mathcal{Q}_{n_e, n'_e}^{(y)} \quad (20)$$

and

$$J_{jk}^{(z)} = \int d\mathbf{r} z^2 \Phi_j^*(\mathbf{r}) \Phi_k(\mathbf{r}) = \frac{\hbar}{m\omega_z} \delta_{n_e, n'_e} \mathcal{Q}_{n_z, n'_z}^{(z)} , \quad (21)$$

with

$$\mathcal{Q}_{n_e, n'_e}^{(y)} = \int_0^\infty \xi d\xi \exp(-\xi) \mathcal{L}_{n_e}^{(\Lambda)}(\xi) \mathcal{L}_{n'_e}^{(\Lambda)}(\xi) \quad (22)$$

and

$$\mathcal{Q}_{n_z, n'_z}^{(z)} = \int_{-\infty}^\infty \zeta^2 d\zeta \exp(-\zeta^2) \mathcal{H}_{n_z}(\zeta) \mathcal{H}_{n'_z}(\zeta) , \quad (23)$$

respectively. Finally, these functions are expressed in terms of the standard Hermite $\mathcal{H}_{n_z}(\zeta)$ and associated Laguerre polynomials $\mathcal{L}_{n_e}^{(\Lambda)}(\xi)$ [see Eqs. (A.7) and (A.8) defined in the new dimensionless variables ξ and ζ , Eq. (A.6)]. The calculation of the Θ_i in Eq. (19) is thus reduced to the determination of the transformation matrices $A_{\mu\nu}$ and the calculation of the simple integrals (22) and (23). They can be solved analytically through the recurrence relations of the orthogonal polynomials.

To study the correspondence between quantum and classical description we will carry out our study with a WS potential (14) having a relatively sharp edge (small diffuseness) and a large depth, in order to simulate in this way the classical motion of particles inside a box of spheroidal shape.

IV. SEMICLASSICAL APPROACH

Within the POT, both the s.p. energy of the system and the MI can be subdivided into an average part and a semiclassical shell correction, as this has been done for the MI in Eq. (10). It is then possible [19, 23] to express these shell components through one another

$$\delta\Theta_{\text{scl}} \approx m \left\langle \frac{r_{\perp}^2}{\varepsilon} \right\rangle_{\text{ETF}} \delta E_{\text{scl}} , \quad (24)$$

where δE_{scl} is the semiclassical energy shell correction, with a proportionality coefficient given by

$$\left\langle \frac{r_{\perp}^2}{\varepsilon} \right\rangle_{\text{ETF}} = \frac{\int d\varepsilon \varepsilon \int d\mathbf{r} d\mathbf{p} (r_{\perp}^2/\varepsilon) g_{\text{ETF}}(\mathbf{r}, \mathbf{p}; \varepsilon)}{\int d\varepsilon \varepsilon \int d\mathbf{r} d\mathbf{p} g_{\text{ETF}}(\mathbf{r}, \mathbf{p}; \varepsilon)} , \quad (25)$$

and $g_{\text{ETF}}(\mathbf{r}, \mathbf{p}; \varepsilon)$ is the ETF approximation to the semiclassical level-density distribution $g_{\text{scl}}(\mathbf{r}, \mathbf{p}; \varepsilon) = \partial f_{\text{scl}}(\mathbf{r}, \mathbf{p})/\partial\varepsilon$ and $f_{\text{scl}}(\mathbf{r}, \mathbf{p})$ the Fermi distribution in

phase-space [19, 24]. For the simple TF approach, one has

$$g_{\text{scl}}(\mathbf{r}, \mathbf{p}; \varepsilon) \approx g_{\text{TF}}(\mathbf{r}, \mathbf{p}; \varepsilon) = \delta(\varepsilon - H(\mathbf{r}, \mathbf{p})) , \quad (26)$$

with $H(\mathbf{r}, \mathbf{p})$ being the classical Hamiltonian. Notice that the relationship $H(\mathbf{r}, \mathbf{p}) = \varepsilon$ appears in Eq. (25) after integration over the momentum \mathbf{p} due to the δ function in (26) and its derivative with respect to ε (see Ref. [24]). In the derivation of Eq. (24) for the MI shell correction $\delta\Theta_{\text{scl}}$ the improved stationary phase (periodic orbit) condition for the evaluation of integrals over the phase space variables \mathbf{r} and \mathbf{p} has been used [19, 20, 22–24, 30, 31]. Within the POT, the PO sum for the energy shell corrections δE_{scl} writes for an arbitrary potential well [12–14, 16, 19, 20, 22, 29–31]

$$\delta E_{\text{scl}} = d_s \sum_{\text{PO}} \frac{\hbar^2}{t_{\text{PO}}^2} \delta g_{\text{PO}}(\varepsilon_F) , \quad (27)$$

where $t_{\text{PO}} = M t_{\text{PO}}^{M=1}(\varepsilon_F)$ is the period of particle motion along the PO (taking into account its repetition number M) and $t_{\text{PO}}^{M=1}$ is the period of the particle motion along the primitive ($M = 1$) PO, evaluated at the Fermi energy $\varepsilon = \varepsilon_F$. For the shell correction to the semiclassical level density, one can write

$$\delta g_{\text{scl}}(\varepsilon) \cong \sum_{\text{PO}} \delta g_{\text{PO}}(\varepsilon) , \quad (28)$$

where

$$\delta g_{\text{PO}}(\varepsilon) = \mathcal{A}_{\text{PO}}(\varepsilon) \cos \left(\frac{S_{\text{PO}}(\varepsilon)}{\hbar} - \frac{\pi}{2} \mu_{\text{PO}} - \phi \right) , \quad (29)$$

with \mathcal{A}_{PO} being the density amplitude. In the argument of the cosine function the phase S_{PO} corresponds to the action integral for the PO (or the family of POs), μ_{PO} is the Maslov index (see Ref. [41]) and ϕ is an additional phase that depends on the dimension of the problem and the degeneracy of the considered orbits [16, 19, 20, 31]. The Fermi energy ε_F is determined by the particle-number conservation condition (5), that can be written in the form

$$N = d_s \int_0^{\varepsilon_F} d\varepsilon g(\varepsilon) , \quad (30)$$

where $g(\varepsilon)$ is the total level density. One needs to solve this equation to determine the Fermi energy as function of the particle number, since ε_F is needed in Eq. (27) to obtain the energy shell correction δE_{scl} . If one were to use the exact level density $g(\varepsilon)$ in (30), one would obtain a step function for the Fermi energy as function of the particle number. Using the semiclassical level density

$$g_{\text{scl}}(\varepsilon) \approx g_{\text{ETF}}(\varepsilon) + \delta g_{\text{scl}}(\varepsilon) \quad (31)$$

with $\delta g_{\text{scl}}(\varepsilon)$ given by Eq. (28) with (29), similar discontinuities would appear. To avoid such a behavior,

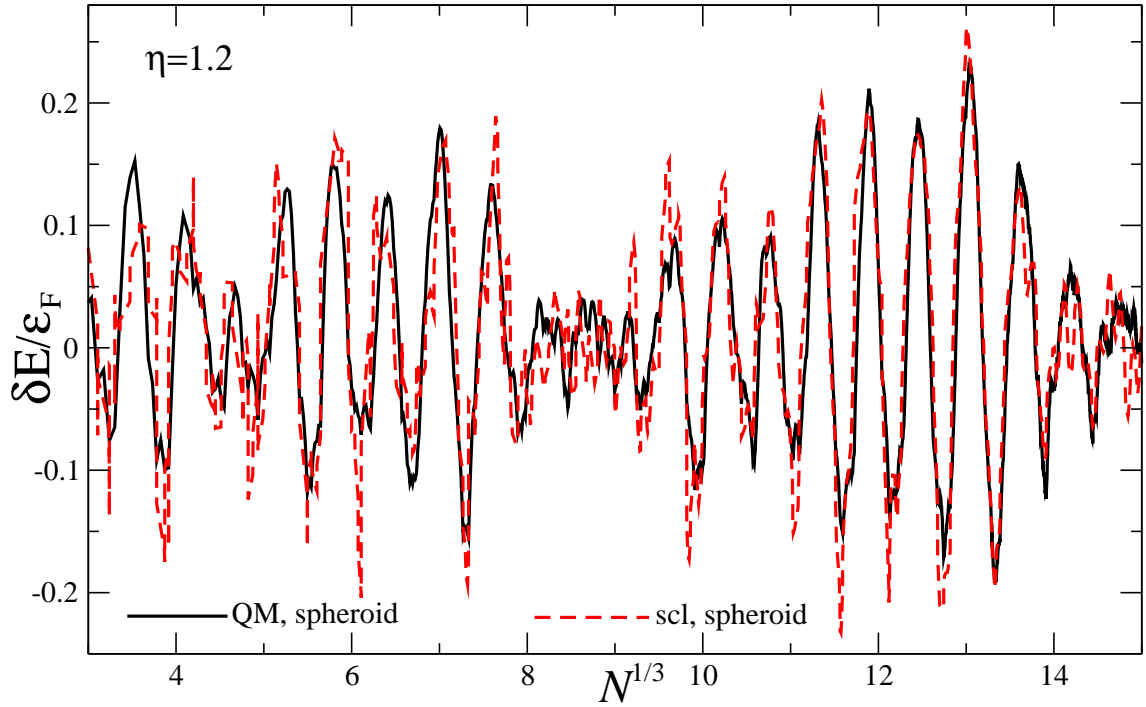


FIG. 1. Quantum-mechanical (solid black) and semiclassical (dashed red line) shell-correction energies δE (in units of the Fermi energy ε_F) as function of the cubic root $N^{1/3}$ of the particle number, for a spheroidal cavity at deformation $\eta = 1.2$.

one can apply some kind of Gauss averaging on the level density $g(\varepsilon)$ used in Eq. (30), or, what amounts to the same, on the quantum level density, with, however, a width parameter γ_0 , much smaller than in the case of a shell-correction calculation by the Strutinsky smoothing, namely with $\gamma_0 \ll \hbar\Omega$, i.e. much smaller than the distance between major shells, but still larger than the energy distance between neighboring s.p. levels. Because of the slow convergence of the PO sum in Eq. (28), it is, however, more convenient to use in (30) the exact level density $g(\varepsilon)$, averaged as explained above, to determine the smooth function $\varepsilon_F(N)$ representing the Fermi energy as function of the particle number N .

The rapid convergence of the PO sum in Eq. (27) is ensured by the factor in front of the density component δg_{PO} , a factor which is inversely proportional to the square of the period of motion t_{PO} along the considered PO. Only POs with reasonably short periods which occupy a large enough phase-space volume will therefore contribute. Let us mention at this point, that the energy shell correction δE in Eq. (24) is, of course, through Eq. (30), function of the particle number N . For the ETF average $\langle r_{\perp}^2/\varepsilon \rangle_{\text{ETF}}$, Eq. (25), one can simply use its TF approximation, which gives [19, 23, 24] for the spheroidal cavity the expression through the semi-axes a and b of Eq. (15):

$$\langle \frac{r_{\perp}^2}{\varepsilon} \rangle_{\text{ETF}} \approx \frac{a^2 + b^2}{3\varepsilon_F}. \quad (32)$$

Expressed in units of the classical (TF), i.e. the rigid-

body MI,

$$\Theta_{\text{TF}} = m (a^2 + b^2) \frac{N}{5}, \quad (33)$$

one obtains for the MI shell correction, Eq. (24),

$$\frac{\delta\Theta_{\text{scl}}}{\Theta_{\text{TF}}} = \frac{5 \delta E_{\text{scl}}}{3N\varepsilon_F}. \quad (34)$$

V. DISCUSSION OF SHELL EFFECTS

When calculating the energy shell corrections δE for a system of N particles in a cavity of spheroidal deformation, one obtains some regular oscillations as function of $N^{1/3}$ which are presented in Fig. 1. This calculation has been carried out, using both the quantum-mechanical (QM) and a semiclassical (scl) resolution of the problem, for a spheroidal deformation, with a ratio of semiaxis (see Eq. (16)) of $\eta = 1.2$, i.e. for a rather small deformation. A solid agreement is obtained between both these methods over a very large range of particle numbers as shown in the figure, where the energy shell correction is displayed in units of the Fermi energy ε_F . In our calculations the Fermi energy ε_F was fixed so as to obtain the desired particle number N through Eq. (30), as explained in the previous section. It is not astonishing that the agreement is less pronounced for small particle numbers N where the number of s.p. states becomes gradually too small to carry out the Strutinsky smoothing procedure

with some reasonable accuracy. The deep minima (large negative shell corrections in Fig. 1) correspond to the closed major shells (MS) that appear in nuclei as well as in metallic clusters and that are, for the here considered potential, well reproduced in both the quantum and the semiclassical calculations.

Fig. 2 shows a comparison of the shell corrections to the energy (a) and the MI (b) as functions of the particle number variable, $N^{1/3}$, for a WS potential of spheroidal shape. This potential is chosen to have a constant radius $R_0 = r_0 N^{1/3}$ (with $r_0 = 1.14$ fm), for a fixed particle number $N = 250$ (corresponding approximately to the center of the Fermium ($Z = 100$) isotopic chain), which means that the radius R_0 is fixed in our calculations to a constant value $R_0 = 7.18$ fm. Since in the case of the spheroidal cavity, the spectrum is calculated in the dimensionless variable $k_i R_0$, where $k_i = \sqrt{2m\varepsilon_i}/\hbar$ with ε_i being the energy spectrum of the cavity, this dimensionless variable is independent of the specific value of the radius R_0 . One could therefore, for a comparison of Fig. 2 with the results of the spheroidal cavity (see e.g. Refs. [23, 24]) formally consider both systems to have the same fixed radius R_0 . Note also that the plateau condition of the Strutinsky smoothing procedure for the spheroidal cavity is obtained in the dimensionless $k_i R_0$ spectrum, in contrast to the WS problem where this condition has to be satisfied in the energy shell-correction calculation by averaging over the energy spectrum ε_i with a Gaussian width parameter $\gamma \approx 14 - 24$ MeV and a correction polynomial of degree $M \approx 6 - 10$.

The shell components δE and $\delta\Theta$ of respectively the energy and the MI, shown in panel (a) and (b) of Fig. 2, are calculated by the standard SCM as functions of the nucleon number variable, $N^{1/3}$, in a WS potential well with a depth $V_0 = -300$ MeV, a diffuseness $\alpha = 0.2$ fm and a fixed radius $R_0 = r_0 N^{1/3} = 7.18$ fm ($r_0 = 1.14$ fm, $N = 250$) i.e. with a fixed s.p. spectrum. We have chosen a small diffuseness α and a large depth V_0 for the WS-type potential in order to verify the quantum relationship (2) for this potential, now close to a spheroidal cavity, by comparing it with the semiclassical relationship derived analytically [19, 22–24] for any potential well, in particular for the spheroidal cavity (see Eq. (24)).

It should be made clear from the very beginning that one is not going to obtain for the here considered WS mean-field potential the same quality of correspondence between energy and MI shell components as that had been the case for the harmonic-oscillator potential well [22, 25]. This is mainly due to the fact that the harmonic oscillator Hamiltonian is one of the very few cases (like the free particle) where the second order expansion of the action in the integration over the phase-space variables by the stationary-phase method yields an *exact* result since higher than second-order terms are simply absent. The profound reason of such a full quantization is the complete degeneracy of the POs with the largest value

of the degree of symmetry ¹ $\mathcal{K} \leq 4$ in three dimensions [13, 14, 42], like for the Coulomb potential, but in contrast to other integrable spherical ($\mathcal{K} \leq 3$) and spheroidal ($\mathcal{K} \leq 2$) cavities. This is certainly not the case for the partially non-integrable WS potential and one is not going to expect a strict proportionality between energy and MI shell corrections as predicted on the semiclassical level by Eq. (24). The best one can hope for is that such a correspondence can be established on the level of major shell or major sub-shell structures.

We have found that one is not able to choose α smaller than $\alpha \approx 0.2$ fm because then the expansion of the WS eigenfunctions in the HO basis states becomes badly convergent, and would require a prohibitive number of major shells n_{HO} in the HO spectrum to be taken into account. Note also that there is a difference in the plateau conditions for the calculation of the MI shell corrections $\delta\Theta$ found from the s.p. sum in Eq. (18) as compared to the energy shell correction calculation. The reason is that the quantities Θ_i , Eq. (19), which take the role of a “s.p. spectrum” in Eq. (18), differ from the energy spectrum ε_i by the coefficients $A_{\mu\nu}$ from the expansion (A.1) of the WS eigenfunctions in the deformed HO basis. One also finds a relatively significant increase of the number n_{HO} of shells in the HO basis that need to be taken into account for the calculation of the MI shell component $\delta\Theta$ ($n_{\text{HO}} \gtrsim 14$) as compared to the energy shell correction δE where a value of $n_{\text{HO}} \sim 10$ turns out to be sufficient. This also leads to somewhat different values of the Strutinsky smoothing parameters ($\gamma \approx 20$, $M \approx 6$ for the energy shell correction versus $\gamma \approx 14$, $M \approx 12$ for the MI shell component). These Strutinsky averaging parameters are found about the same for the whole region of particle numbers $N^{1/3}$ shown in Fig. 2

Another problem that we encounter lies in the fact that there is no *reasonable* plateau condition for “billiard” (cavity) potentials, (even for the energy shell correction) when averaging over the energy spectrum ε_i . As well known and mentioned above, one rather needs, in the case of a spheroidal cavity, to consider the wave numbers k_i instead of the energy spectrum to obtain a well pronounced plateau (see, e.g., Refs. [16, 23, 24, 29–31]). On the other hand, the energy spectrum ε_i is used in the averaging procedure for the HO potential [30]. If one now decreases the diffuseness α of the WS potential from a value of $\alpha \approx 0.6$ fm, realistic for a nuclear mean field, to a value of $\alpha \approx 0.2$ fm and simultaneously increases the depth of the potential well from about -50 MeV to -300 MeV, one makes that potential resemble a spheroidal cavity. Being then able to compare our quantum WS results with the result of the semiclassical calculation for that cavity, one has to find some reasonable choice for α in

¹ The symmetry (or degeneracy) parameter \mathcal{K} of a family of POs is the number of single-valued integrals of a particle motion of fixed energy, which determines in a unique way the action integral of the whole family along the PO [13, 14, 20, 29, 31].

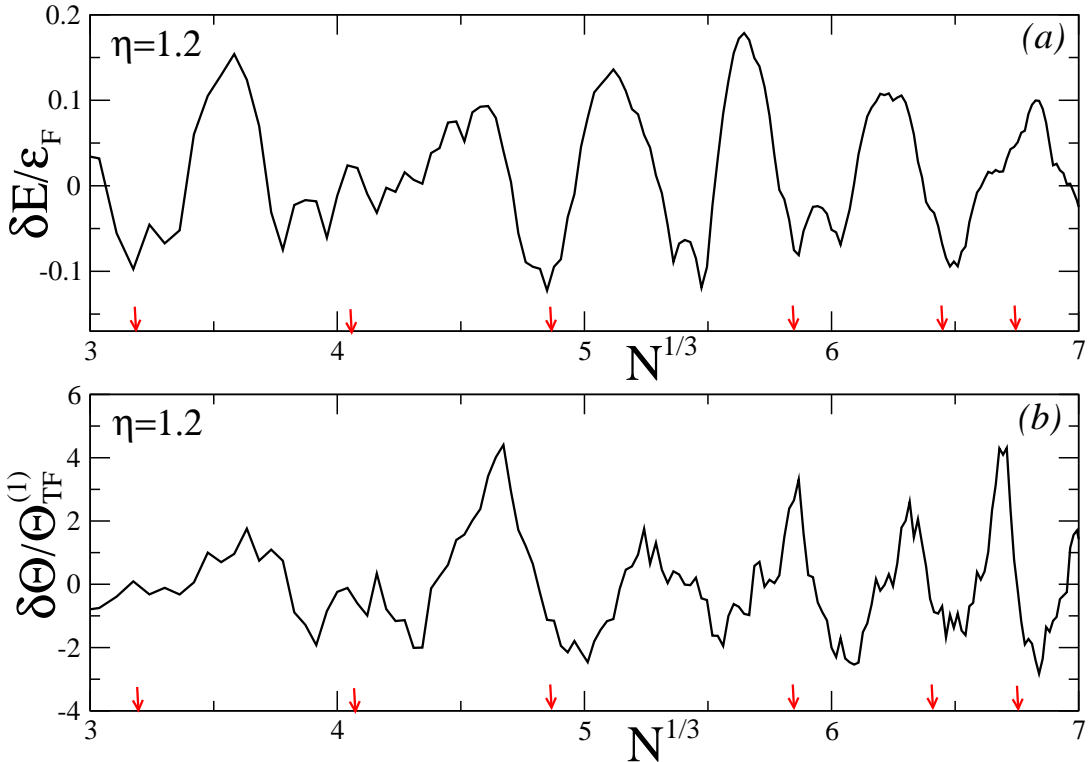


FIG. 2. Quantum-mechanical energy and MI shell corrections, obtained respectively in units of the Fermi energy ε_F and those of the TF MI per particle $\Theta_{\text{TF}}^{(1)} = \Theta_{\text{TF}}/N$, with Θ_{TF} given by Eq. (33), are presented as functions of the particle number variable $N^{1/3}$, at the same deformation ($\eta = 1.2$) as the spheroidal cavity in Fig. 1 but now for a WS potential (see text). Small red arrows indicate MS closures, as taken from Fig. 3 (c).

order to be able to still satisfy the Strutinsky plateau condition for the average over the energy spectrum. Such a compromise is achieved in Fig. 2, for the parameters of the WS potential well as indicated above, at values of the particle number variable $N^{1/3}$ between 3 and 7 corresponding to particle numbers in the range $30 \lesssim N \lesssim 340$.

In the POT calculations presented in Fig. 1 for the spheroidal cavity, the Fermi energy $\varepsilon_F(N)$ changes of course with the particle number N through Eq. (30). The MI shell corrections in the WS potential, as presented in Fig. 2, on the other hand, are divided by the TF MI per particle, Eq. (33), that scales with the particle number N , $\Theta_{\text{TF}}^{(1)} = \Theta_{\text{TF}}(N)/N = m(a^2 + b^2)/5$. Here one should take into account that, because of using a constant radius R_0 , this TF MI Θ_{TF} is proportional to the particle number N . Nevertheless, when displaying the ratio $\delta\Theta/\Theta_{\text{TF}}^{(1)}$ as function of $N^{1/3}$, as we do in Fig. 2, one obtains a result that has essentially a constant amplitude. Note that the amplitude of $\delta E_{\text{scl}}/\varepsilon_F$ as function of $N^{1/3}$ is also almost constant with an almost constant spacing between major shells (see Fig. 2(a)). One has to note that the family of periodic orbits that gives the main contribution to the semiclassical shell-correction amplitude for the case of the spheroidal cavity is enhanced as compared to the case of the WS potential. Due to the integrability of the

spheroidal cavity, the symmetry parameter \mathcal{K} (see footnote 1 above) is larger there, for the orbits with highest degeneracy ($\mathcal{K} = 2$), as compared to those in the axially-symmetric WS potential, where the orbits with highest degeneracy only have $\mathcal{K} = 1$ for the same deformation. Therefore, the shell-correction amplitudes, Eq. (24), of both the energy and the MI are expected to be enhanced by a factor $N^{1/6}$ for the spheroidal square-well as compared to those for the WS potential, (see Refs. [20, 31]).

The shell correction $\delta\Theta_{\text{scl}}$, Eq. (24), of the MI turns out to be much smaller than the classical TF (rigid-body) component², similar to the energy shell-correction δE compared to the corresponding TF term. Many important physical phenomena, such as fission isomerism or high-spin physics depend, however, dramatically on these shell effects. Shell effects are also expected to play a major role for the magnetic susceptibility, as a reaction of a system of charged particles to a magnetic field, which are expressed by exactly the same type of equa-

² Please recall, when comparing the MI shell correction $\delta\Theta$ with the TF MI Θ_{TF} , Eq. (33), that the quantity $\delta\Theta/\Theta_{\text{TF}}^{(1)}$ which is plotted in Fig. 2 (b) still needs to be divided by the particle number N , in order to judge the relative importance of both these quantities.

tions as we have for the MI, as mentioned above. There, the oscillating (shell) components are going relatively to be largely enhanced as compared to the case of the MI, studied here (see, e.g., Ref. [18]). Our non perturbative approach for the MI shell corrections can, of course, be applied for larger rotational frequencies and larger deformations (e.g. for $\eta \sim 2.0$) where PO bifurcations will play a dominant role, like in the case of a deformed harmonic oscillator [22, 25, 26].

The somewhat “*non professional*” looking behavior of the shell corrections in Fig. 1 calls for some explanation. When plotting the energy shell correction $\delta E_{\text{scl}}/\varepsilon_F$, deduced from Eq. (27), as function of the Fermi energy ε_F , one obtains a smooth curve without any sharp peaks, which, however, appear as soon as one substitutes the function $\varepsilon_F(N)$, as explained in detail in section IV. The same behavior is, of course, and for the same reasons, also observed for the MI shell corrections. One can therefore conclude that the spikes observed for the MS structure in Fig. 1 do not have any profound physical meaning, but have their origin simply in the quantum structure of our s.p. spectrum. For obvious reasons, we have therefore used a slightly larger Gaussian width parameter for the averaging of the level density $g(\varepsilon)$ in Eq. (30), to make appear more clearly the major-shell structure (MSS) versus the sub-shell structure (SSS) in the study of the proportionality between $\delta\Theta$ and δE as derived in the semiclassical approximation in Eqs. (24) and (27), respectively. Notice that the factor $1/t_{\text{PO}}^2$ in Eq. (27), with the time period t_{PO} of the particle motion along the PO, enhances, for the rather small deformation presented in the example of Fig. 1 and in Refs. [19, 22–26], shorter meridian and equatorial POs in the spheroidal cavity. The contributions of longer newborn three-dimensional and hyperbolic orbits, on the other hand, are contributing very little for such small deformations as compared to the meridian and equatorial orbits [29, 31]. They are, however, expected to be more important at larger deformations. All these properties differ significantly from the results of the classical perturbation theory of Ref. [28], where equatorial orbits, e.g., do not contribute at all.

In order to be able to test over several major shells the correspondence (2) of the MS structure that appear as functions of $N^{1/3}$ in the shell corrections of the MI $\delta\Theta$ and the energy δE a large enough interval of particle numbers needs to be considered. Notice that the semiclassical relationship (24) converges asymptotically to the quantum results, a convergence which is the better the larger the particle number N . On the other hand, when increasing the number n_{HO} of HO basis shells, one needs to check the plateau condition for each value of n_{HO} , and, in fact, for each particle numbers. This plateau condition for the particle number N is, however, much less sensitive for large N values ($N^{1/3} \cong 3 - 7$). It also turns out that, whereas the plateau for the energy shell correction is rather wide, we only find a much shorter plateau for the MI shell correction $\delta\Theta$ as function of the averaging parameters γ and M . A satisfactory plateau is, however,

always obtained as long as the particle number N is not too small. One observes, indeed, that the interval in the particle-number variable $N^{1/3}$ is much smaller for the case of the WS potential (Fig. 2) as compared to the one of the cavity (Fig. 1). The reason for this restriction lies in the fact that, in order to obtain a good accuracy for the Strutinsky plateau condition, two conditions need to be met: the number of particles needs to be sufficiently large so that a reasonably large number of s.p. states can be included in the Strutinsky procedure, a fact that automatically excludes the case of very small particle numbers. When the particle number becomes very large, on the other hand, so that s.p. states close to the continuum are populated, these continuum effects will require a more refined treatment, which is very involved. Within the restricted interval of the particle-number variable $N^{1/3}$ between 3 and 7 we are, however, on the *safe side* and can obtain a good statistical accuracy over several major shells in the particle number dependence not only for the energy δE , but also for the MI shell correction $\delta\Theta$.

To better appreciate the interconnection between the energy shell correction δE and the corresponding MI shell correction $\delta\Theta$, it is important to be able to differentiate the MSS from the ones corresponding to SSS of the N particle system. To this purpose we show in Fig. 3 the level-density shell correction which determines both of these quantities. As explained in section IV in connection with determination of the Fermi energy ε_F through Eq. (30), a Gauss averaging needs to be applied to the level density $g(\varepsilon)$ in order to avoid discontinuities in the function $\varepsilon_F(N)$. In order to be able to differentiate MSS from SSS structures, we need, however, to use a larger value of the parameter γ for a convolution with a Gaussian. While a value of $\gamma_0 \approx 0.2$ MeV has to be used in the Strutinsky smoothing of the level density in Eq. (30), we have used values of γ_{sh} between 2 or 3 (for the SSS) and 6 (for the MSS) to reveal respectively the SS and the MS structures as this can be seen in Fig. 3, where MS closures are indicated in panel (c) through small red arrows. It is interesting to observe that in the major shell located at $N^{1/3}$ values between 4.9 and 5.8 a sub-shell closure can be identified at $N^{1/3}$ around 5.3 as found in the level-density shell-correction of Fig. 3 (a) and (b), and which corresponds to a sub-shell closure for δE and $\delta\Theta$ in the vicinity of $N^{1/3} \approx 5.5$ (see Fig. 2 (a) and (b)).

For the level-density shell corrections δg_γ , the plateau parameters ($\gamma \cong 19$ MeV and $M \cong 6$) are the same as for the energy shell-correction calculations (Fig. 2 (a)). The additional Gaussian width parameter γ_{sh} needs on one hand to be substantially larger than the distance between neighboring s.p. levels, but, on the other hand, much smaller than the distance $\hbar\Omega$ between major shells, not to wash out the main sub-shell or major shell structure completely in the here studied range of the particle number variable $N^{1/3}$ between 3 and 7. Please recall that when calculating the Fermi energy ε_F so as to satisfy the particle-number condition, Eq. (30), we have used in section IV a Gaussian distribution with a width param-

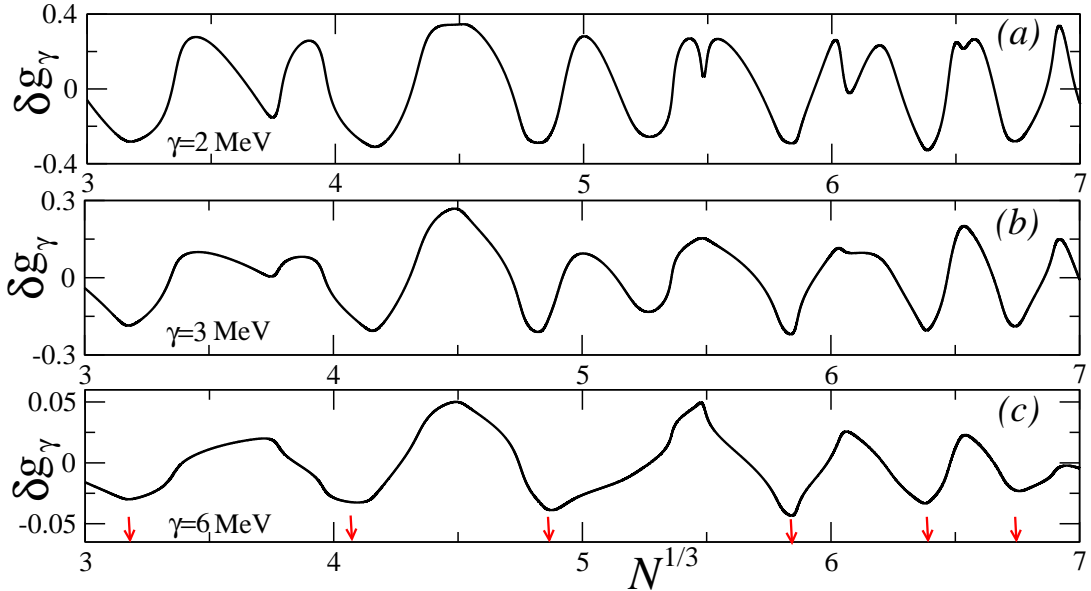


FIG. 3. Level-density shell corrections δg_γ (in units of MeV^{-1}) as function of the particle number variable $N^{1/3}$ obtained for the WS potential of Fig. 2 by a Gauss averaging with a width parameter γ_{sh} as indicated in the different panels. Red arrows in the panel (c) indicate the MS closures.

parameter γ_0 of the order $\gamma_0 \lesssim 0.2$ MeV in order to somehow smear out step-function discontinuities. In the same way one evidences by choosing γ_{sh} somewhat larger, sub-shell structures (with $\gamma_{sh} = 2$ or 3) as shown in Fig. 3 (a) and (b) or major-shell structures (with $\gamma_{sh} = 6$) as demonstrated in Fig. 3 (c).

Even though the agreement of the variation, as function of the particle-number variable $N^{1/3}$, of the shell components $\delta E/\varepsilon_F$ and $\delta\Theta/\Theta_{\text{TF}}^{(1)}$ is not as striking as this was the case for the harmonic oscillator potential [22, 25], we still confirm Eq. (24) in terms of major-shell structures. Indeed, as already pointed out above, one should not expect to obtain the same quality of agreement, like a strict proportionality in Eq. (24), between these two quantities in a quantum calculation as performed here, for the simple reason that one is not able then to use the stationary phase approximation of the semiclassical approach, valid asymptotically in the limit of large particle numbers (see Refs. [19, 23, 24]). Nevertheless, one notices, indeed, the presence of several MS closures in the range of $N^{1/3}$ values between 3 and 7 for which a relatively close correspondence between the energy and the MI shell correction is observed in terms of major shells. For large particle numbers, i.e. in the limit when $N^{1/3} \gg 1$, semiclassical methods are particularly well adapted, but we encounter problems with the Strutinsky shell-correction method for large particle numbers where $N^{1/3} \gtrsim 7$ ($N \gtrsim 340$), because, for the mean-field potential that we have been gradually filling, the Fermi energy comes close to the continuum of the s.p. spectrum, which is always difficult to handle. For smaller particle numbers, in particular below $N^{1/3} \lesssim 3$,

on the other hand, shell corrections δE or $\delta\Theta$ are not well defined because then the number of s.p. states becomes too small to carry out the Strutinsky smoothing procedure with a good accuracy, as already pointed out at the beginning of the present section. Note that in the comparison of the quantum shell correction δE for a smooth-edge WS potential (Fig. 2) with the semiclassical result for an infinitely deep spheroidal square-well potential (Refs. [23, 24]), one needs to take into account different boundary conditions. Indeed, these lead to an additional shift of the Maslov phase in δE , Eqs. (27–29), for the spheroidal cavity, as compared with the case of the WS potential [16, 31, 41], as suggested by the small shift discrepancy of the last two major shells in Fig. 2 (a) and (b). Another interesting and nontrivial example is the MS structure located in $N^{1/3}$ between 4 and 5, which has a different SSS in δE (Fig. 2(a)) and $\delta\Theta$ (Fig. 2(b)).

As becomes evident from Sec. IV a qualitative agreement can be observed between the semiclassical POT and the quantum results for both the deformed spheroidal cavity and a deep and almost sharp-edged WS potential. We are thus able to establish a *statistical correspondence* of our relation (24) between the shell contributions $\delta\Theta$ and δE on the level of the resolution of major-shell structures, as this was already observed more strictly for the harmonic oscillator potential [22, 25].

VI. CONCLUSIONS

The shell corrections to the moment of inertia are determined through the generalized rigid-body MI for equi-

librium rotations beyond the quantum perturbation expansion. We have shown that, for a WS potential of a small spheroidal deformation, the semiclassical relation (24) between energy and moment-of-inertia shell corrections approximately holds for the major shell structure and is in qualitative agreement with the quantum result. This correspondence between δE and $\delta\Theta$ is observed for a relatively sharp edged WS potential of spheroidal shape. A more systematic investigation of the relationship between these two shell corrections and a comparison between semiclassical and quantum results is on our agenda. It will be of particular interest to carry out this study in a large range of deformations, since at larger deformations the bifurcation phenomenon is expected to play an important role [14, 20, 22, 29, 31, 41]. We confirm the fundamental property common in general to all finite Fermi systems that the “major-shell structure” of $\delta\Theta$ is generated by the one of the energy shell corrections δE through the inhomogeneity of the distribution of single-particle states near the Fermi surface.

As for further perspectives, one could think of applying our semiclassical theory to the shell corrections of other transport coefficients, such as the inertia and friction parameters, that play an important role, e.g. in the description of the fission process [43, 44]. We also plan to apply our approach to nuclear systems with a more realistic surface diffuseness [20, 45] within the nuclear collective dynamics, in particular involving magic nuclei, where the above discussed effects should be strongest. Using a more realistic Hamiltonians with more generally deformed mean-field potentials and diffused edges, one could, in addition, study the bridge bifurcations due to an unlocal symmetry restoration [45], as explained in the review [20]. In this connection it is obvious that our POT results could be extremely interesting for calculations of shell effects in the magnetic susceptibilities in quantum dots [18, 35].

One of the most attractive applications of the semiclassical periodic-orbit theory, however, seems to us its extension to the spin-orbit and pairing interactions [46–49], and the study of their influence on the collective vibrational and rotational excitations in heavy deformed neutron-rich nuclei (see e.g. Ref. [50]). To compare our theoretical predictions for the moment of inertia with the experimental data on rotational bands in well deformed nuclei, one could think of combining the smooth ETF MI with the corresponding PO shell corrections.

Acknowledgement

The authors gratefully acknowledge J.P. Blocki for many fruitful discussions. We are also very grateful for many creative discussions with K. Arita, R.K. Bhaduri, M. Brack, S.N. Fedotkin, S. Frauendorf, A.N. Gorbatchenko, F.A. Ivanyuk, V.M. Kolomietz, M. Matsuo, K. Matsuyanagi, V.A. Plujko, and A.I. Sanzhur. One of us (A.G.M.) is very grateful for the nice hospitality extended to him during his working visits of the National Centre for Nuclear Research in Otwock-Swierk/Warsaw, the Hu-

bert Curien Institute of the Strasbourg University, the University of Regensburg/Germany, and the Physics Department of the Nagoya Institute of Technology/Japan. Many thanks also go to the Japanese Society for the Promotion of Sciences for their financial support, Grant No. S-14130. This work was also supported by the budget program “Support for the development of priority areas of scientific research” of the National Academy of Sciences of Ukraine (Code No. 6541230).

Appendix A: Harmonic oscillator basis

For the quantum calculations of the MI and the energy shell corrections in the spheroidal WS potential (14), one can perform the diagonalization procedure through an expansion of the WS eigenfunctions $\psi_i(\mathbf{r})$ in the basis of a deformed harmonic oscillator [40]:

$$\psi_i(\mathbf{r}) = \sum_j A_{ij} \Phi_j(\mathbf{r}) . \quad (\text{A.1})$$

The HO basis states Φ_j are defined in cylindrical coordinates $\{\varrho, \varphi, z\}$ ($x = \varrho \cos\varphi$, $y = \varrho \sin\varphi$, z) as

$$\Phi_j(\mathbf{r}) = |j\rangle = |n_z n_\varrho \Lambda\rangle = \mathcal{R}_{n_\varrho}^{(\Lambda)}(\varrho) \mathcal{Z}_{n_z}(z) \phi_\Lambda(\varphi) , \quad (\text{A.2})$$

where n_z , n_ϱ , and Λ are the quantum numbers of the state and

$$\mathcal{R}_{n_\varrho}^{(\Lambda)}(\varrho) = \left(\frac{2m\omega_\perp}{\hbar} \right)^{1/2} \exp(-\xi/2) \mathcal{L}_{n_r}^{(\Lambda)}(\xi) , \quad (\text{A.3})$$

$$\mathcal{Z}_{n_z}(z) = \left(\frac{m\omega_z}{\hbar} \right)^{1/4} \exp(-\zeta^2/2) \mathcal{H}_{n_z}(\zeta) , \quad (\text{A.4})$$

$$\phi_\Lambda(\varphi) = (2\pi)^{-1/2} \exp(i\Lambda\varphi) , \quad (\text{A.5})$$

with

$$\xi^{1/2} = (m\omega_\perp/\hbar)^{1/2} \varrho = b_\perp \varrho , \quad \zeta = (m\omega_z/\hbar)^{1/2} z = b_z z . \quad (\text{A.6})$$

The frequencies ω_\perp and ω_z of the axially-symmetric HO basis are connected, as usual, by the volume conservation condition $\omega_\perp^2 \omega_z = \omega_0^3$, with $\omega_\perp/\omega_z = q$ being the deformation parameter of the basis, i.e. $\omega_\perp = \omega_0 q^{1/3}$ and $\omega_z = \omega_0 q^{-2/3}$. It is convenient to use dimensionless variables as we have done through Eqs. (A.6) by introducing an inverse length $b_0 = \sqrt{m\omega_0/\hbar}$ as a parameter of the HO basis (for nuclear systems with $\mathcal{N} \sim 200 - 300$ considered in our study, one obtains together with $\hbar\omega_0 \approx 50 \text{ MeV}/\mathcal{N}^{1/3}$ a value of $b_0 \approx 0.45 \text{ fm}^{-1}$) and consequently corresponding inverse lengths $b_\perp = b_0 q^{1/6}$ and $b_z = b_0 q^{-1/3}$. The functions $\mathcal{L}_{n_r}^{(\Lambda)}(x)$ and $\mathcal{H}_{n_z}(x)$ in

Eqs. (A.3) and (A.4) are related to the standard generalized Laguerre $L_n^{(\Lambda)}(x)$, and Hermite $H_n(x)$ polynomials by

$$\mathcal{L}_n^{(\Lambda)}(x) = \left(\frac{n!}{(n + \Lambda)!} \right)^{1/2} x^{\Lambda/2} L_n^{(\Lambda)}(x), \quad (\text{A.7})$$

and

$$\mathcal{H}_n(x) = (2^n n! \pi^{1/2})^{-1/2} H_n(x). \quad (\text{A.8})$$

The functions $\mathcal{L}_{n_r}^{(\Lambda)}(x)$ and $\mathcal{H}_n(x)$ obey orthogonality relations similar, up to constants, to those of the Laguerre, $L_n^{(\Lambda)}(x)$, and Hermite, $H_n(x)$, polynomials themselves [40]. One thus obtains the following relation for the transformation coefficients A_{ij} in Eq. (A.1):

$$\sum_j A_{ij}^2 = 1. \quad (\text{A.9})$$

[1] D.R. Inglis, Phys. Rev. **96** (1954) 1059; Phys. Rev. **97**, 701 (1955); D.R. Inglis, Phys. Rev. **103**, 1786 (1956).

[2] A. Bohr and B. Mottelson, Mat. Fys. K. Dan. Vidensk. Selsk, **30**, 1 (1955).

[3] J.G. Valatin, Proc. R. Soc. London **A238**, 132 (1956).

[4] A. Bohr and B. Mottelson, *Nuclear Structure* (Benjamin, New York, 1975) Vol. II.

[5] P. Ring, P. Schuck, *The Nuclear Many-Body Problem* (Springer-Verlag, New York, Heidelberg, Berlin, 1980).

[6] V.M. Strutinsky, Nucl. Phys. **A95**, 420 (1967); V.M. Strutinsky, Nucl. Phys. **A122**, 1 (1968).

[7] M. Brack, L. Damgaard, A.S. Jensen, H.C. Pauli, V.M. Strutinsky, and C.Y. Wong, Rev. Mod. Phys. **44**, 320 (1972).

[8] V.V. Pashkevich and S. Frauendorf, Sov. J. Nucl. Phys. **20**, 588 (1975).

[9] I.N. Mikhailov, K. Neergard, V.V. Pashkevich, and S. Frauendorf, Sov. J. Part. Nucl. **8**, 550 (1977).

[10] M. Gutzwiller, J. Math. Phys. **12**, 343 (1971).

[11] M. Gutzwiller, *Chaos in Classical and Quantum Mechanics* (Springer-Verlag, New York, 1990).

[12] V.M. Strutinsky, *Nukleonika (Poland)* **20**, 679 (1975).

[13] V.M. Strutinsky and A.G. Magner, Sov. J. Part. Nucl. **7**, 138 (1976).

[14] V.M. Strutinsky, A.G. Magner, S.R. Ofengenden, and T. Dössing, Z. Phys. **A283**, 269 (1977).

[15] A.G. Magner, V.M. Kolomietz, and V.M. Strutinsky Sov. J. Nucl. Phys. **28**, 764 (1978).

[16] M. Brack and R.K. Bhaduri, *Semiclassical Physics. Frontiers in Physics* No. 96, 2nd ed. (Westview Press, Boulder, CO, 2003).

[17] V.M. Kolomietz, A.G. Magner, and V.M. Strutinsky, Sov. J. Nucl. Phys. **29**, 758 (1979).

[18] S. Frauendorf, V.M. Kolomietz, A.G. Magner, and A.I. Sanzhur Phys. Rev. B **58**, 5622 (1998).

[19] A.G. Magner, D.V. Gorpichenko, and J. Bartel, Phys. At. Nucl. **80**, 122 (2017).

[20] A. G. Magner, M. V. Koliesnik, and K. Arita, Phys. Atom. Nucl. **79**, 1067 (2016).

[21] L. D. Landau, E. M. Lifshitz, *Statistical Physics* (Pergamon, 1980).

[22] A.G. Magner, D.V. Gorpichenko, and J. Bartel, Phys. At. Nucl. **77**, 1229 (2014).

[23] D.V. Gorpichenko, A.G. Magner, J. Bartel, and J.P. Blocki, Phys. Scr. **T90**, 114008 (2015).

[24] D.V. Gorpichenko, A.G. Magner, J. Bartel, and J.P. Blocki, Phys. Rev. C, **93**, 024304 (2016).

[25] A.G. Magner, A.S. Sitzdikov, A.A. Khamzin, and J. Bartel, Phys. Rev. C **81**, 064302 (2010).

[26] A. G. Magner, A. S. Sitzdikov, A. A. Khamzin, J. Bartel, and A. M. Gzhebinsky, Nucl. Phys. and At. Energy **10**, 239 (2009); Int. J. Mod. Phys. E **19**, 735 (2010); Yad. Fiz. **73**, 1442 (2010) [Phys. Atom. Nucl. **73**, 1398 (2010)].

[27] S.C. Creagh, Ann. Phys. (NY), **248**, 60 (1996).

[28] M.A. Deleplanque, S. Frauendorf, V.V. Pashkevich et al., Phys. Rev. C **69**, 044309 (2004).

[29] A.G. Magner, K. Arita, S.N. Fedotkin, and K. Matsuyanagi, Prog. Theor. Phys. **108**, 853 (2002).

[30] A.G. Magner, K. Arita, and S.N. Fedotkin, Prog. Theor. Phys. **115**, 523 (2006).

[31] A.G. Magner, Y.S. Yatsyshyn, K. Arita, and M. Brack, Phys. At. Nucl. **74**, 1445 (2011).

[32] K. Bencheikh, P. Quentin, and J. Bartel, Nucl. Phys. A **571**, 518 (1994).

[33] M. Brack, C. Guet, and H.B. Häkansson, Phys. Rep. **123**, 275 (1985).

[34] A.G. Magner, S.M. Vydroug-Vlasenko, H. Hofmann, Nucl. Phys. A **524**, 31 (1991).

[35] K. Richter, D. Ulmo, and R.A. Jalabert, Phys. Rep. **276**, 1 (1996).

[36] A.M. Gzhebinsky, A.G. Magner, and S.N. Fedotkin, Phys. Rev. C **76**, 064315 (2007).

[37] A.B. Migdal, *Qualitative Methods in Quantum Theory* (W. A. Benjamin, Reading, MA, 1977).

[38] J. P. Blocki, A. G. Magner, and I. S. Yatsyshyn, Nucl. Phys. and At. Energy **11**, 239 (2010); Int. J. Mod. Phys. E **20**, 292 (2011); Int. J. Mod. Phys. E, 2012.

[39] J. Blocki, J. Skalski, and W. J. Swiatecki, Nucl. Phys. A **594**, 137 (1995).

[40] J. Damgaard, H.-C. Pauli, V.V. Pashkevich, and V.M. Strutinsky, Nucl. Phys. A **135**, 432 (1969).

[41] A.G. Magner and K. Arita, Phys. Rev. E **96**, 042206 (2017).

[42] A.G. Magner, Sov. J. Nucl. Phys. **28**, 764 (1978).

[43] H.J. Krappe, K. Pomorski, Lecture notes in Physics **838**, Springer, Heidelberg, London, New York, 2012.

[44] J. Bartel, B. Nerlo-Pomorska, K. Pomorski, A. Dobrowolski, Comp. Phys. Com. **241**, 139 (2019).

[45] K. Arita, Phys. Scr. **92**, (2017).

[46] M. Brack and P. Quentin, Nucl. Phys. A **361**, 3 (1981).

- [47] Ch. Amann and M. Brack, J. Phys. A: Math. Gen. **35**, 6009 (2002).
- [48] M. Brack, Ch. Amann, M. Pletyukhov, and O. Zaitsev, Int. J. Mod. Phys. E**13**, 19 (2004).
- [49] M. Brack and X. Roccia, Int. J. Mod. Phys. E**19**, 725 (2010).
- [50] S. Frauendorf, *Pairing at high spin*, Ch.39 in book: *50 Years of BCS in Nuclear Physics*, ed. by R. Broglia and V.V. Zelevinsky (World Science Publ. Singapore, 2013).